Journal of the Nigerian Mathematical Society
Vol. 40, Issue 3, pp. 339-351, 2021

EFFECT OF SURFACE ROUGHNESS ON ELECTRO-MAGNETO-HYDRODYNAMIC FLOW IN A ROUGH CURVED CHANNEL

NNAMDI FIDELIS OKECHI

ABSTRACT. For a flow through an applied electric and magnetic field, the effect of surface roughness on the curved walls confining the flow is presented. The roughness is considered as a small perturbation to the smooth walls of the curved channel. The analytical expression of the pertinent volumetric flow rate is obtained through boundary perturbation method, where the amplitude of the prescribed roughness is taken as the perturbation parameter. The study indicates that the overall effect of rough curved walls decreases as the electro-magnetic force increases over the viscous force.

Keywords and phrases: Hartmann number, rough walls, phase difference, radius of curvature, volumetric flow rate
2010 Mathematical Subject Classification: 34E10, 76D05, 76W05

1. INTRODUCTION

Roughness on the boundaries of a channel may be considered as deviations from the ideal surface of the channel. The presence of roughness has been found to significantly influence the flow through conduits characterized by either artificially imposed or naturally induced roughness. Through the studies carried out by several researchers, the effects of channel roughness have been investigated, where different types of roughness have been described by different functions. Flow in a rough straight channel was studied by Wang [1]. Phan-Thien [2] examined Stokes flows in channels and pipes with stationary random surface roughness. The flow pattern and pressure drop in rough microchannels were analyzed by Wang and Wang [3]. The instability of flow in a rough channel was discussed by Floryan [4]. The modelling of surface roughness effects on Stokes flow in circular pipes was considered by Song et al. [5]; periodic roughness of sinusoidal, triangular, and rectangular morphologies

Received by the editors March 28, 2021; Revised: November 11, 2021; Accepted: November 26, 2021
www.nigerianmathematicalsociety.org; Journal available online at https://ojs.ictp.it/jnms/

were considered and their effects on the low Reynold number flow field and pressure drop were analyzed. Duan and Muzychka [6] studied the effect of roughness on flow in microtubes. The authors presented the effects of no-slip and slip rough wall conditions on the incompressible flow. The analysis of electro-magneto-hydrodynamic flow through a rough microchannel was given by Buren et al. [7]. Related studies can also be found in the following articles, namely, [8]-[15]. On the other hand, flows through rough curved channels have been modelled and studied by Okechi and Asghar ([16]-[19]) for various flow orientations. The authors studied the behaviour of rough curved channel flows, relative to smooth curved channel flows. The inherent analyses indicate that the effects of the enclosing rough walls depend substantially on the flow orientations, with respect to the structure of the roughness.

In the present work, an incompressible flow through a rough curved channel is studied, such that the flow traverses an applied electric field and a radially imposed magnetic field. The electric field vector is constant, whereas, the magnetic field vector is a function of the channel radius of curvature and the space variable in the direction of the field. The objective of this work is to examine the effects of roughness and the electro-magnetic force on the volumetric flow rate and to ascertain the variation in the flow characteristics in comparison to that of a smooth curved channel, of the same radius of curvature and subjected to the same electro-magnetic force. A quantitative relation between the flow rate in a rough curved channel and that of a smooth curved channel will be determined, and the percentage change in the flow rate due to the presence of roughness will be calculated.

In section 2, the physical model and the perturbation analysis are given. The mathematical model of the problem is provided and the description of the wall roughness is specified. The analysis is carried out for an arbitrary phase difference between the two rough curved walls. Through perturbation analysis, the expression of the volumetric flow rate is obtained. Section 3 entails the results and discussion via graphical and tabular representations. Finally, the concluding remarks are provided in section 4.

2. PHYSICAL MODEL AND ANALYSIS

Consider a flow driven along the x-direction, perpendicular to an electric field $\mathbf{E} = (0, 0, E)$ and a magnetic field $\mathbf{B} = (0, \frac{Bk}{y+k}, 0)$ imposed in the z-direction and y- direction, respectively, as shown

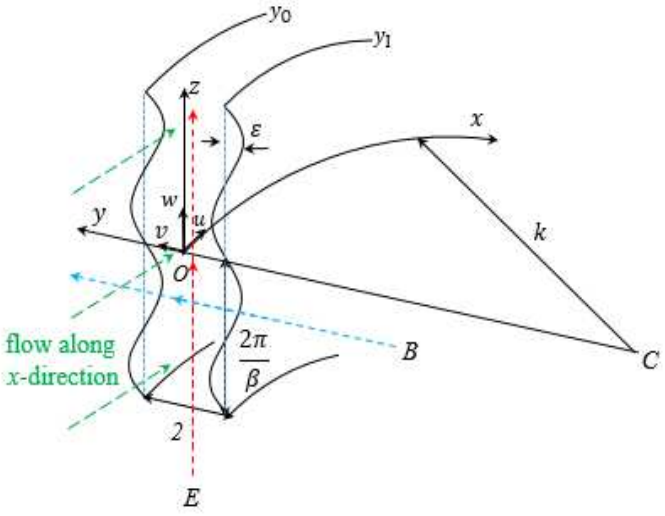

Fig. 1. The normalized flow geometry.

Fig. 1, where $k > 0$ is the channel radius of curvature. The governing equations for the incompressible flow; including the equations of mass and momentum conservations can be written, respectively, in vector form as

$$\begin{aligned} \nabla \cdot \mathbf{u} &= \mathbf{0}, \\ \rho \frac{d\mathbf{u}}{dt} &= -\nabla p + \mu \Delta \mathbf{u} + \mathbf{J} \times \mathbf{B}, \end{aligned} \tag{1}$$

where ρ, μ and p, are the fluid density, dynamic viscosity, and pressure, respectively, while t is the time. The material derivative, the gradient vector and the Laplacian are given by $\frac{d}{dt}$, ∇, and Δ, respectively. The electro-magnetic force known as the Lorentz force is defined by the vector $\mathbf{J} \times \mathbf{B}$, where $\mathbf{J} = \sigma(\mathbf{E} + \mathbf{u} \times \mathbf{B})$ is the current density and σ is the fluid conductivity. For a unidirectional steady flow generated by pressure gradient $-\partial_x p = G$, with velocity vector $\mathbf{u} = (u, 0, 0)$, the governing equations for the flow problem can be expressed, in the curvilinear coordinates ([16]-[20]) as;

$$\begin{aligned} (y+k)^2 \partial_y \left((y+k)^{-1} \partial_y (y+k)\, u \right) + (y+k)^2 \partial_{zz} u \\ -k \left(k\sigma B^2 u - \sigma (y+k) EB \right) = -k (y+k) G, \end{aligned} \tag{2}$$

where $\partial_j g$ is the derivative of the function g with respect to the variable j. Suppose the curved walls, separated by a distance $2a$ are rather rough, we may define the roughness of the walls by the wave functions $y_{\mathrm{O}} = a + b \sin\left(\frac{2\pi z}{\lambda}\right)$ and $y_{\mathrm{I}} = -a + b \sin\left(\frac{2\pi z}{\lambda} + \varsigma\right)$, for the outer and the inner rough walls, respectively, where b is

the amplitude, λ is the wavelength and ς is the phase difference between the rough curved walls. Thus, the no-slip wall conditions for the flow read;

$$u = \begin{cases} 0, & y = y_{\mathrm{O}} = a + b\sin(\frac{2\pi z}{\lambda}) \\ 0, & y = y_{\mathrm{I}} = -a + b\sin(\frac{2\pi z}{\lambda} + \varsigma). \end{cases} \tag{3}$$

Normalizing the lengths by a, and the velocity is by $\frac{a^2 G}{\mu}$, Eqs. (2) and (3) can be rewritten in the dimensionless form

$$(y+k)\partial_y\left((y+k)\partial_y u\right) + (y+k)^2\partial_{zz}u - \beta^2 u = -(\mathrm{N}+1)k(y+k),$$
$$u = \begin{cases} 0, & y = y_{\mathrm{O}} = 1 + \varepsilon\sin(\alpha z) \\ 0, & y = y_{\mathrm{I}} = -1 + \varepsilon\sin(\alpha z + \varsigma), \end{cases} \tag{4}$$

where $\beta^2 = k^2\mathrm{Ha}^2 + 1$, $\mathrm{Ha} = Ba\sqrt{\frac{\sigma}{\mu}}$ is the flow Hartmann number; $\mathrm{N} = \sigma\frac{EB}{G}$ is a parameter due to the electric field; ε is the dimensionless amplitude and $\alpha = \frac{2\lambda a}{\lambda}$ is the wavenumber which specifies the spatial frequency of the roughness. Now, for a small amplitude of the rough walls relative to the channel width ($\varepsilon << 1$), we can express the solution of the boundary valued problem (BVP), Eq. (4), as;

$$u = u_0 + \varepsilon u_1 + \varepsilon^2 u_2 + O(\varepsilon^3). \tag{5}$$

$$\begin{aligned} u(1 + \varepsilon\sin(\alpha z), z) &= u(1) + \varepsilon\sin(\alpha z)u_y(1, z) \\ &+ \frac{1}{2}\varepsilon^2\sin^2(\alpha z)u_{yy}(1, z) + O(\varepsilon^3) = 0, \end{aligned} \tag{6}$$

$$\begin{aligned} u(-1 + \varepsilon\sin(\alpha z + \varsigma), z) &= u(-1) + \varepsilon\sin(\alpha z + \varsigma)u_y(-1, z) \\ &+ \frac{1}{2}\varepsilon^2\sin^2(\alpha z + \varsigma)u_{yy}(-1, z) + O(\varepsilon^3) = 0, \end{aligned} \tag{7}$$

On substituting Eqs. (5)-(7) in Eq. (4), we get the following boundary value problems. Now, for the zeroth-order ($O(\varepsilon^0)$), the BVP is

$$\begin{aligned} (y+k)\partial_y\left((y+k)\partial_y u_0\right) - \beta^2 u_0 &= -(\mathrm{N}+1)k(y+k), \\ u_0(1) = 0, \qquad u_0(-1) &= 0. \end{aligned} \tag{8}$$

The solution of Eq. (8) is given as

$$u_0(y) = c_0(y+k)^{\beta} + b_0(y+k)^{-\beta} + k(\mathrm{N}+1)(y+k)/k^2\mathrm{Ha}^2, \tag{9}$$

where

$$c_0 = \frac{k(\mathrm{N}+1)\left((k-1)(k+1)^{-\beta} - (k+1)(k-1)^{-\beta}\right)}{k^2\mathrm{Ha}^2\left((k+1)^{\beta}(k-1)^{-\beta} - (k-1)^{\beta}(k+1)^{-\beta}\right)}, \tag{10}$$

and

$$b_0 = \frac{k(\mathrm{N}+1)\left((k+1)(k-1)^{\beta} - (k-1)(k+1)^{\beta}\right)}{k^2\mathrm{Ha}^2\left((k+1)^{\beta}(k-1)^{-\beta} - (k-1)^{\beta}(k+1)^{-\beta}\right)}. \tag{11}$$

For the first-order ($O(\varepsilon^1)$), the BVP is

$$\begin{aligned}(y+k)\partial_y\left((y+k)\partial_y u_1\right) - ((y+k)^2\partial_{zz} + \beta^2)u_1 = 0,\\ u_1(1,z) = -\sin(\alpha z)\partial_y u_0(1),\\ u_1(-1,z) = -\sin(\alpha z + \varsigma)\partial_y u_0(-1).\end{aligned} \tag{12}$$

Solving Eq. (12), the exact periodic solution is

$$u_1(y,z) = \sum_{\gamma=1}^{2} U_\gamma(y)\sin(\alpha z + (\gamma-1)\pi/2), \tag{13}$$

where

$$U_\gamma(y) = c_\gamma I_\beta\big(\alpha(y+k)\big) + b_\gamma K_\beta\big(\alpha(y+k)\big), \tag{14}$$

$$c_\gamma = \frac{(2-\gamma)K_\beta\big(\alpha(k-1)\big)U_\gamma(1) - K_\beta\big(\alpha(k+1)\big)U_\gamma(-1)}{I_\beta\big(\alpha(k+1)\big)K_\beta\big(\alpha(k-1)\big) - K_\beta\big(\alpha(k+1)\big)I_\beta\big(\alpha(k-1)\big)}, \tag{15}$$

and

$$b_\gamma = \frac{I_\beta\big(\alpha(k+1)\big)U_\gamma(-1) - (2-\gamma)I_\beta\big(\alpha(k-1)\big)U_\gamma(1)}{I_\beta\big(\alpha(k+1)\big)K_\beta\big(\alpha(k-1)\big) - K_\beta\big(\alpha(k+1)\big)I_\beta\big(\alpha(k-1)\big)}. \tag{16}$$

For the second-order ($O(\varepsilon^2)$), the BVP is given as

$$\begin{aligned}(y+k)\partial_y\big((y+k)\partial_y u_2\big) - ((y+k)^2\partial_{zz} + \beta^2)u_2 = 0,\\ u_2(1,z) = -\frac{1}{2}\sin^2(\alpha z)\partial_{yy}u_0(1) - \sin(\alpha z)\partial_y u_1(1,z),\\ u_2(-1,z) = -\frac{1}{2}\sin^2(\alpha z + \varsigma)\partial_{yy}u_0(-1) - \sin(\alpha z + \varsigma)\partial_y u_1(-1,z).\end{aligned} \tag{17}$$

From Eq. (17), the exact solution is found to be

$$u_2(y,z) = U_3(y) + \sum_{\gamma=4}^{5} U_\gamma(y)\sin(2\alpha z + (\gamma-4)\pi/2). \tag{18}$$

Eq. (18) consist of a combination of periodic and non-periodic parts in z. Since the periodic part of Eq. (18) will no contribute to the volumetric flow rate, we are only interested in the non-periodic part, thus, we have the solution

$$u_2(y,z) = U_3(y) = c_3(y+k)^{\beta} + b_3(y+k)^{-\beta}, \tag{19}$$

where

$$c_3 = \frac{U_3(1)(k-1)^{-\beta} - U_\beta(-1)(k+1)^{-\beta}}{(k+1)^\beta(k-1)^{-\beta} - (k-1)^\beta(k+1)^{-\beta}}, \tag{20}$$

$$b_3 = \frac{U_3(-1)(k+1)^\beta - U_3(1)(k-1)^\beta}{(k+1)^\beta(k-1)^{-\beta} - (k-1)^\beta(k+1)^{-\beta}}. \tag{21}$$

Note that, the functions I_β and K_β are modified Bessel functions of order β, and of the first and second kind, respectively. The normalized volumetric flow rate Q for the flow problem can be obtained from the integral defined as ([15]-[18])

$$Q = \frac{\alpha}{2\pi}\int_0^{\frac{2\pi}{\alpha}}\int_{y_{\text{I}}}^{y_{\text{O}}} u dy dz \tag{22}$$

The expression of Eq. (22) can be expanded up to second-order in ε to get

$$\begin{aligned} Q = &\int_{-1}^{1} u_0 dy + \varepsilon\frac{\alpha}{2\pi}\int_0^{\frac{2\pi}{\alpha}}\int_{-1}^{1} u_1 dy dz \\ &+ \varepsilon^2\frac{\alpha}{2\pi}\bigg(\int_0^{\frac{2\pi}{\alpha}}\int_{-1}^{1} u_2 dy dz \\ &+ \int_0^{\frac{2\pi}{\alpha}} (\sin(\alpha z)u_1(1) - \sin(\alpha z+\varsigma)u_1(-1))dz \\ &+ \frac{1}{2}\int_0^{\frac{2\pi}{\alpha}} (\sin^2(\alpha z)\partial_y u_0(1) - \sin^2(\alpha z+\varsigma)\partial_y u_0(-1))dz\bigg) \\ &+ O(\varepsilon^4). \end{aligned} \tag{23}$$

Substituting the velocity expression in Eq. (23) it becomes:

$$Q = q(1+\varepsilon^2\chi) + O(\varepsilon^4). \tag{24}$$

Eq. (24) is the quantitative relation between Q and q, where

$$\begin{aligned} q = \frac{1}{k^2\text{Ha}^2}\bigg(&b_0(\beta+1)((k-1)^{1-\beta} - (k+1)^{1-\beta}) \\ &+ c_0(\beta-1)((k+1)^{1+\beta} - (k-1)^{1+\beta}) + 2k^2(\text{N}+1)\bigg), \end{aligned} \tag{25}$$

and

$$\chi = \frac{1}{q}\Bigg(\frac{\beta}{4}c_0\big((k+1)^{1-\beta} - (k-1)^{1-\beta}\big) + b_0\big((k-1)^{-1-\beta} - (k+1)^{-1-\beta}\big)\Big) + \frac{1}{2}\big(c_1 I_\beta(\alpha(k+1)) + b_1 K_\beta(\alpha(k+1)) - (c_1 I_\beta(\alpha(k-1)) + b_1 K_\beta(\alpha(k-1)))\cos(\varsigma) - (c_2 I_\beta(\alpha(k-1)) + b_2 K_\beta(\alpha(k-1)))\sin(\varsigma)\big) + \frac{1}{k^2 \mathrm{Ha}^2}\big((\beta+1)b_3((k-1)^{1-\beta} - (k+1)^{1-\beta}) - (\beta-1)c_3((k-1)^{1+\beta} - (k+1)^{1+\beta})\big)\Bigg). \tag{26}$$

Now, $q = q(k, \mathrm{N}, \mathrm{Ha})$ is the flow rate through the smooth curved channel in the absence of roughness, while $\chi = \chi(\alpha, \varsigma, k, \mathrm{N}, \mathrm{Ha})$ is the roughness function which specifies the effect of the surface roughness on the flow.

3. RESULTS AND DISCUSSION

In this section, the variations of both the volumetric flow rate q through a smooth curved channel and the volumetric flow rate Q through the rough curved channel are discussed as functions of the pertinent flow parameters. Further to that, the percentage change in the volumetric flow rate due to the wall roughness is discussed. Fig. 2 illustrates the variation of the function q with the Hartmann number Ha of the flow. It can be noticed that, for a smooth curved channel, q decreases continuously with Ha, for a given k. Physically, this trend is attributed to the presence of the electro-magnetic force, which opposes the flow in the stream wise direction. In Fig. 3, the analytical result in the previous section is validated: For a given k, large enough, the present result corresponds to the flow rate of Poiseuille flow in a smooth straight channel (which is indicated by the dashed line [20]) in the absence of both electric and magnetic fields.

In Fig. 4, we have given the variation of the roughness function χ with the alignment of the curved walls defined by the phase difference ς, for each Ha. This shows that χ increases with ς. However, with increasing Ha, χ decreases in magnitude and ceases to vary with ς for sufficiently large Ha. This means that for sufficiently

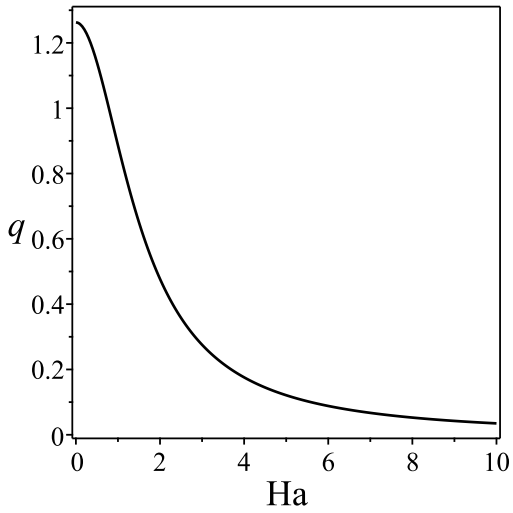

Fig. 2. Variation of flow rate q through a smooth curved channel with Ha, when $k = 1.3$ and N $= 1$.

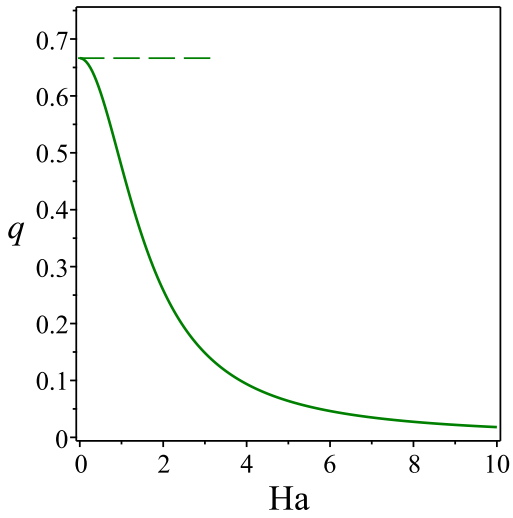

Fig. 3. Variation of flow rate q through a smooth curved channel with Ha, when $k = 15$ and N $= 0$.

large Ha, the effect of the alignment of the two rough curved walls on the volumetric flow rate Q is negligible.

More also, from Fig. 4, it can be clearly understood that the maximum and minimum values of χ occur at $\varsigma = \pi$ and $\varsigma = 0$, respectively. Therefore, in the next figures, the variations of χ with Ha for different α and k are discussed for these extrema (i.e. $\varsigma = \pi$

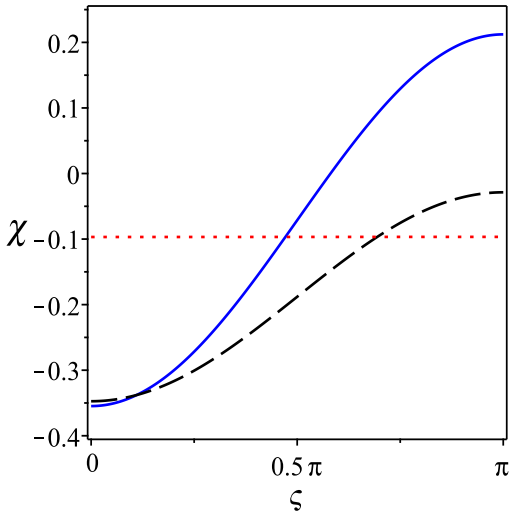

Fig. 4. Variation of the roughness function χ with ς, when $k = 2$, N $= 1$, Ha $= 0.5$ (solid lines) Ha $= 1$ (dashed lines) and Ha $= 5$ (dotted lines)

and $\varsigma = 0$), keeping in mind that $\chi > 0$ and $\chi < 0$ increases and decreases the volumetric flow rate Q, respectively, through Eq. (24). In Fig. 5, for small Ha, the effect of the roughness is significant for any α. While the effect of ς on χ is distinctively obvious for small α, ς ceases to show any distinct effect for large α. This is because, as α increases, the frequency of the roughness increases, thus, the flow resistance due to the confining rough walls becomes increased, consequently. This situation renders the phase difference between the rough curved walls immaterial. Hence, the roughness effect will be the same irrespective of the alignment of rough curved wall. Furthermore, ς loses its effect on the flow as Ha increases, such that, for Ha large enough, χ does not vary with ς, even for small α. At this point, it is important to emphasize that the roughness function changes from $\chi > 0$ to entirely $\chi < 0$, as the parameter α increases. Fig. 6 demonstrates the variation of χ with Ha for different k. This indicates that the roughness effect changes in magnitude with channel radius of curvature. We can observe that the rough curved walls confining the flow will have more decreasing effect on the flow for large Hartmann number, compared to rough straight channel walls.

To determine the percentage change in the volumetric flow rate due to the presence of the roughness, we have provided Tables 1

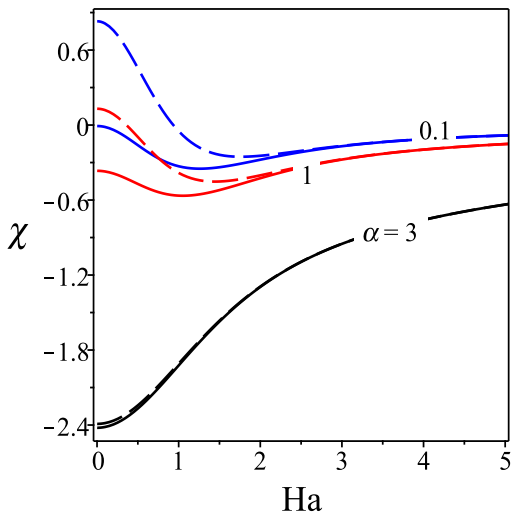

Fig. 5. Variation of the roughness function χ with Ha, for different α, when $k = 1.3$, N $= 1$, $\varsigma = \pi$ (dashed lines) and $\varsigma = 0$ (solid lines).

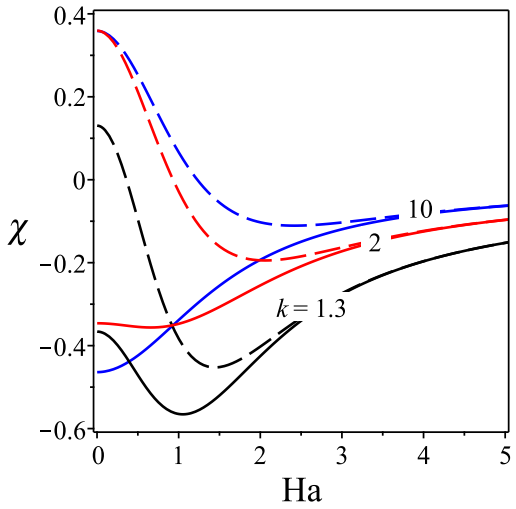

Fig. 6. Variation of the roughness function χ with Ha, for different k, when $\alpha = 1$, N $= 1$, $\varsigma = \pi$ (dashed lines) and $\varsigma = 0$ (solid lines).

and 2. In Table 1, for $\alpha = 0.1$, it is evident that when the phase difference between the rough curved walls is zero, i.e., $\varsigma = 0$, a percentage decrease is obtained, irrespective of the channel radius of curvature k. On the contrary, for $\varsigma > 0$, a percentage increase in

the volumetric flow rate is obtained for each k. More also, the overall percentage change increases in magnitude as we go from $\varepsilon = 0.1$ to 0.15. This demonstrates that the effects of the roughness may become more profound as the roughness amplitude increases relative to the channel width. In Table 2, when $\alpha = 1$, the percentage decrease in the volumetric flow rate extends from $\varsigma = 0$ to both $\varsigma = 0.5\pi$ and $\varsigma = \pi$ (for $k = 2$), whereas, the percentage increase is obtained only at $\varsigma = \pi$ for both $k = 5$ and 10. Like Table 1, the percentage change is also magnified from $\varepsilon = 0.1$ to 0.15 in Table 2. The tables are an indication of the fact that while the flow enhancement maybe possible for $\varsigma > 0$ and sufficiently small α. The tendency of obtaining such enhancement diminishes with increasing α, such that for large value of α, there will only be a percentage decrease in the flow.

Table 1. Percentage change in the volumetric flow rate. $\alpha = 0.1$, N = 1 and Ha = 1.

	$\varepsilon = 0.1$			$\varepsilon = 0.15$		
	$\varsigma = 0$	$\varsigma = 0.5\pi$	$\varsigma = \pi$	$\varsigma = 0$	$\varsigma = 0.5\pi$	$\varsigma = \pi$
$k = 2$	-0.04980	0.20536	0.46050	-0.11205	0.46206	1.03613
$k = 5$	-0.00600	0.31523	0.63648	-0.01350	0.70927	1.43208
$k = 10$	-0.00396	0.32649	0.65701	-0.00891	0.73460	1.47827

Table 2. Percentage change in the volumetric flow rate. $\alpha = 1$, N = 1 and Ha = 1.

	$\varepsilon = 0.1$			$\varepsilon = 0.15$		
	$\varsigma = 0$	$\varsigma = 0.5\pi$	$\varsigma = \pi$	$\varsigma = 0$	$\varsigma = 0.5\pi$	$\varsigma = \pi$
$k = 2$	-0.34756	-0.18812	-0.02858	-0.78201	-0.42327	-0.06431
$k = 5$	-0.33620	-0.13912	0.05819	-0.75645	-0.31302	0.13093
$k = 10$	-0.33827	-0.13610	0.06624	-0.76111	-0.30623	0.14904

4. CONCLUDING REMARKS

In this study, we have examined the effects of roughness on the volumetric flow rate associated with the flow through a rough curved channel subjected to an imposed electric and magnetic fields. The volumetric flow rate has been analyzed. The existence of channel surface roughness may be favourable or not to the flow through such channels, under the circumstances that have been considered here. That is to say, for roughness defined by small wavenumbers, a percentage increase in the flow is possible, since the flow is increased by

the roughness beyond that of smooth curved channel (keeping the same parameters). However, for large wavenumbers, a percentage decrease in the flow is inevitable, irrespective of the alignment of the two rough curved walls. In terms of the applied magnetic field; the effect of the roughness is decreased by the magnetic field compared to when the magnetic field is absent. Therefore, an applied magnetic field can be used to control the influence of the roughness on the volumetric flow rate.

NOMENCLATURE

(x, y, z)	curvilinear coordinate
u	velocity in x-direction
v	velocity in y-direction
v	velocity in z-direction
$\mathbf{u} = (u, v, w)$	velocity vector
a	channel width
k	channel radius of curvature
p	pressure
$\mathbf{B}$	magnetic field
$\mathbf{E}$	electric field
$\mathbf{J}$	current density
Q	volumetric flow rate
Ha	Hartmann number
y_{O}	outer rough boundary
y_{I}	inner rough boundary
μ	dynamic viscosity
ρ	density
ς	phase difference
ε	dimensionless amplitude
σ	electrical conductivity
α	wavenumber
λ	wavelength
χ	roughness function

REFERENCES

[1] C. Y. Wang, *Parallel flow between corrugated plates*, J. Eng. Mech. **102** 1088-1090, 1976.

[2] N. Phan-Thien, *On Stokes flows in channels and pipes with parallel stationary random surface roughness*, Z. Angew. Math. Mech. **61** 193-199, 1981.

[3] H. Wang and Y. Wang, *Flow in microchannels with rough walls: flow pattern and pressure drop*, J. Micromech. Microeng. **17** 586-596, 2007.

[4] J. M. Floryan, *Two-dimensional instability of flow in a rough channel*, Phys. Fluids **17** 044101, 2005.

[5] S. Y. Song, X .H. Yang, F. X. Xin and T. J. Lu, *Modeling of surface roughness effects on Stokes flow in circular pipes*, Phys. Fluids **30** 023604, 2018.
[6] Z. Duan and Y. S. Muzychka, *Effects of corrugated roughness on developed laminar flow in microtubes*, J. Fluid Eng. **130** 031102, 2008.
[7] M. Buren, Y. Jian and L. Chang, *Electromagnetohydrodynamic flow through a microparallel channel with corrugated walls*, J. Phys. D: Appl. Phys. **47** 425501, 2014.
[8] M. Greiner, *An experimental investigation of resonant heat transfer enhancement in grooved channels*, Int. J. Heat Mass Transfer **34** 1383-1391, 1991.
[9] G. Fabbri, *Heat transfer optimization in corrugated wall channels*, Int. J. Heat Mass Transfer **43** 4299-4310, 2000.
[10] N. Ghaddar and A. El-Hajj, *Numerical Study of Heat Transfer Augmentation of Viscous Flow in Corrugated Channels*, Heat Transfer Eng. **43** 35-46, 2000.
[11] A. Garcia, J. Solano, P. Vicente and A. Viedma, *The influence of artificial roughness shape on heat transfer enhancement: Corrugated tubes, dimpled tubes and wire coils*, Appl. Therm. Eng. **35** 196-201, 2012.
[12] H. A. Mohammed, Azher M. Abed and M. A. Wahid, *The effects of geometrical parameters of a corrugated channel with in out-of-phase arrangement*, Int. Commun. Heat Mass Transf. **40** 47-57, 2013.
[13] N. Tokgoz, M. M. Aksoy and B. Sahin, *Investigation of flow characteristics and heat transfer enhancement of corrugated duct geometries*, Appl. Therm. Eng. **118** 518-530, 2017.
[14] N. Tokgoz, T. Tunay and B. Sahin, *Effect of corrugated channel phase shifts on flow structures and heat transfer rate*, Exp. Therm. Fluid Sci. **99** 374-391, 2018.
[15] A. Wakif, A. Chamkha, T. Thumma, I. L. Animasaun and R. Sehaqui, *Thermal radiation and surface roughness effects on the thermo-magneto-hydrodynamic stability of aluminacopper oxide hybrid nanofluids utilizing the generalized Buongiornos nanofluid model*, J. Therm. Anal. Calorim. **143** 1201-1220, 2021.
[16] N. F. Okechi and S. Asghar, *Fluid motion in a corrugated curved channel*, Eur. Phys. J. Plus. **134** 165, 2019.
[17] N. F. Okechi and S. Asghar, *Oscillatory flow in a corrugated curved channel*, Eur. J. Mech. B Fluids **84** 81-92, 2020.
[18] N. F. Okechi and S. Asghar, *Darcy-Brinkman flow in a corrugated curved channel*, Transp. Porous Med. **135** 271-286, 2020.
[19] N. F. Okechi and S. Asghar, *Flow in groovy curved channels with thin gap*, Can. J. Phys. **98** 1108-1118, 2020.
[20] H. Schlichting and K. Gersten, *Boundary layer theory*, Springer-Verlag, Berlin Heidelberg, 2017.
[21] F. M. White, *Viscous Fluid Flow*, McGraw-Hill, New York, 2006.

MATHEMATICS PROGRAMME, NATIONAL MATHEMATICAL CENTRE, ABUJA, NIGERIA
E-mail address: okechinnamdi@hotmail.com